JOURNAL OF AIRCRAFT
Vol. 33, No. 5, September–October 1996

Residual Strength of Panels with Multiple Site Damage

E. J. Moukawsher*
U.S. Coast Guard Repair and Supply Center, Elizabeth City, North Carolina 27909
and
M. B. Heinimann† and A. F. Grandt Jr.‡
Purdue University, West Lafayette, Indiana 47907-1282

This article describes research aimed at predicting the residual strength (RS) of unstiffened aluminum panels that contain multiple site damage (MSD). The initial damage consists of through-the-thickness cracks emanating from a row of holes in the center of a 23-cm- (9-in.-) wide panel. The row of holes is aligned perpendicular to a remote tensile load, and three failure criteria are employed to predict the fracture resistance of the cracked panel. RS tests of 2024-T3 aluminum panels with MSD were conducted to evaluate the analyses. The RS tests validate a failure criterion that includes plastic zone considerations for panels with a lead crack spanning the central holes and with small MSD cracks at other holes. The RS tests also demonstrate that significant loss of strength occurs when MSD cracking exists, even when the cracks are relatively small.

Introduction

THE term multiple site damage (MSD) refers to the existence of simultaneous cracking at various structural locations. Coalescence of such cracks can lead to sudden fracture, and may occur at loads significantly below what would be expected from considering the fracture resistance of single cracks. The MSD phenomenon was the cause of the well-known Aloha Airlines incident of April 28, 1988, in which a 4.5-m- (15-ft-) long section of fuselage structure peeled open in flight, resulting in one death and near loss of the Boeing 737 aircraft.[1] This accident dramatically demonstrated that small cracks, acting together, can have a significant effect on the ability of aircraft structure to resist large lead cracks.[2]

A companion article[3] deals with the influence of MSD on the fatigue life of panels subjected to cyclic tension. A numerical model is developed there for the initiation, growth, and coalescence of cracks along a row of open holes in wide panels that contain various degrees of precracking. The model is compared with the results of fatigue tests conducted on 2024-T3 aluminum specimens, and is shown to give a good estimate of the total fatigue life of specimens containing MSD. While that article focuses on the cyclic portion of the MSD problem, this article deals with the final fracture process. Simple criteria for determining the residual strengths (RS) in unstiffened panels containing MSD are discussed, and then compared with the results of tests conducted on 23-cm- (9-in.-) wide 2024-T3 (bare) aluminum specimens. Although MSD is widely recognized as one of the symptoms of aging aircraft, there is concern that some people within the aircraft industry do not fully appreciate the extent to which MSD can degrade lead crack residual strength.[2] Thus, one goal of these experiments and analyses is to demonstrate the effect that small fatigue cracks (MSD) have on the ability of a structure to withstand fracture from a large lead crack.

The panel geometries of interest here are shown in Fig. 1. The type 1 configuration consists of a large lead crack connecting several holes in the test panel and small radial cracks (MSD) emanating from the remaining holes. The type 2 geometry contains only the central lead crack, with the remaining holes uncracked (no MSD). For reference, a type 3 configuration, which only contained the lead crack, but no other holes or MSD, was also considered. Stress intensity factors for the various lead crack and MSD crack configurations were obtained by a compounding technique described in Refs. 3 and 4.

RS Calculations

When MSD has formed along a row of collinear holes, individual cracks continue to grow until they link-up with other cracks or until the panel fails. Different criteria[2,5–7] may be used to determine the RS, which is defined here as the maximum load a panel can bear before complete failure occurs.

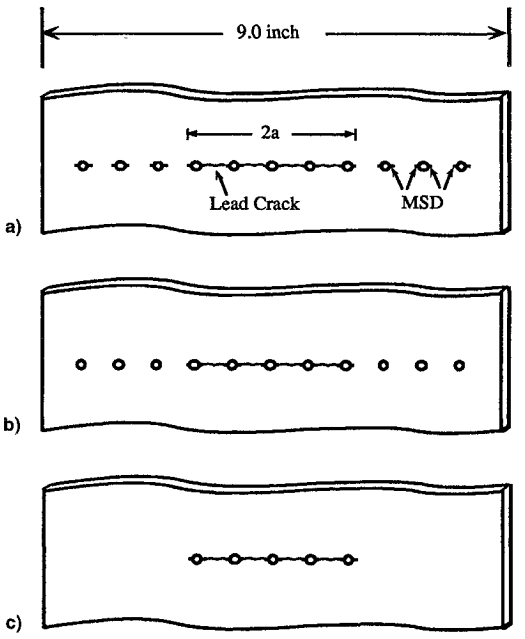

Fig. 1 Schematic representation of the three types of RS specimens: a) type 1 specimen with lead crack and MSD at all holes, b) type 2 specimen with lead crack and holes without MSD, and c) type 3 specimen with lead crack only.

Received Sept. 23, 1995; revision received Feb. 15, 1996; accepted for publication May 15, 1996.

*Chief of Aeronautical Engineering. (Deceased).

†Graduate Research Assistant, 1282 Grissom Hall.

‡Professor, School of Aeronautics and Astronautics, 1282 Grissom Hall. Associate Fellow AIAA.

Although rigorous treatment of the RS problem can involve complex plasticity considerations, this article examines three relatively simple approaches for estimating the RS for panels containing MSD. Those approaches are briefly reviewed next, and then compared with the results of a test program described in the remaining sections.

K-Apparent Criterion

According to linear elastic fracture mechanics (LEFM), there is a critical stress intensity factor value that causes unstable fracture. Known as the fracture toughness K_c, this quantity decreases with increasing specimen thickness, until a limiting value is reached (K_{Ic}, the plane strain fracture toughness). In thin sheets, which allow more yielding than the plane strain conditions found in thicker members, the crack may extend slowly prior to catastrophic fracture. This subcritical crack growth results in the need for a more complete fracture criterion, such as the R-curve, J-integral, or crack tip opening displacement approaches.[6,8] Although LEFM may not apply for the thin 2024-T3 test specimens employed here, it was decided to determine how well the RS in the MSD panels could be predicted with simple fracture toughness concepts. First, an effective fracture toughness was determined for the type 3 specimens by loading the panel until complete failure occurred. The load at failure P_C was recorded and the stress intensity factor at failure was computed. Since subcritical crack growth is difficult to measure experimentally, the initial crack length and the maximum load prior to rapid fracture was chosen to compute K_c. This calculation only approximates K_c and is referred to here as K_{app} (*K*-apparent). Unlike K_c, K_{app} is not strictly a material property, but can vary with different geometries and crack configurations.[8-10]

The following equation was used to determine K_{app} for the center cracked type 3 specimens shown in Fig. 1[11]:

$$K_{app} = P_c\sqrt{\pi a}\beta_w/WB \tag{1}$$

Here, W is the specimen width, B is the specimen thickness, P_c is the applied load at fracture, a is the half-crack length, and β_w is the secant width correction factor given by Eq. (2)[11]:

$$\beta_w = \sqrt{\sec(\pi a/W)} \tag{2}$$

To determine the predicted failure load for the type 1 specimens by this criterion, the lead crack and MSD stress intensity factor solutions described in Refs. 3 and 4 were used to determine the remotely applied load that would produce a stress intensity factor at the central lead crack tip equal to or greater than the measured type 3 K_{app}.

Net Section Yield Criterion

The cross-sectional area available to distribute tensile loads across a collinear row of holes is reduced as MSD cracks propagate from the holes and the net section stress increases. One estimate for the failure load $P_{C\,net}$ is that which causes the net section stress to equal or exceed the tensile yield stress σ_{ys} for the material. For the type 1 panels shown in Fig. 1, this relationship can be expressed as follows:

$$P_{C\,net} = \sigma_{ys}(W - 2a - nd - n_{msd}L)B \tag{3}$$

Here, W is the panel width, a is the half-crack length of the central lead crack, n is the number of holes (not in lead crack), d is the average hole diameter, L is the average MSD crack length, n_{msd} is the number of MSD cracks, B is the panel thickness at the row of holes, and σ_{ys} is the tensile yield strength.

Ligament Yield Criterion

The *K*-apparent and net section yield criteria for determining the failure load do not take into account the loss of panel strength because of crack tip plasticity effects, and could overestimate RS when one considers a relatively large central lead crack bounded on either side by holes with small MSD cracks (as in the type 1 specimens). The plastic zone in front of the large central crack will extend much more rapidly than the zone in front of the MSD cracks, and plasticity associated with the lead crack will control the overall failure of the panel. Figure 2 schematically illustrates this scenario for one of the type 1 panel configurations. As the plastic zone ($2R_2$) for the central lead crack (a_2) extends under load, it reaches a point where it meets the plastic zone from the nearest neighboring MSD crack (a_1). When this occurs, the ligament yield criterion assumes that the two cracks will link up with the lead crack unzipping across the row of holes in a near instantaneous fashion. This mode of failure was proposed by Swift[2,5] as an intuitive approximation of observed failure in panels with MSD, and applies only to the type 1 specimens considered here.

Specimen failure is predicted when the plastic zones in front of the crack tips associated with holes 1 and 2 of Fig. 1 touch. Expressed mathematically, this occurs when the distance t in Fig. 2 is given by Eq. (4):

$$t = 2R_1 + 2R_2 \tag{4}$$

Here, t is the crack tip separation, $2R_1$ is the plastic zone diameter in front of MSD crack a_1, and $2R_2$ is the plastic zone diameter in front of lead crack a_2.

The radius of the plastic zone for the MSD and central lead cracks can be approximated by the well-known Irwin plastic zone estimate[8]:

$$R_y = (1/2\pi)(K/\sigma_{flow})^2 \tag{5}$$

Here, R_y is the plastic zone radius, K is the stress intensity factor at the crack tip under consideration, and σ_{flow} is the flow stress defined as the average of the tensile ultimate and yield stresses.[2]

It should be noted that in Swift's original description of his ligament yield criterion,[2,5] he interpreted Eq. (5) as the plastic zone diameter rather than the plastic zone radius. That application is consistent with Irwin's original plastic zone estimate, although later interpretations[8] of Irwin's plastic zone have suggested that Eq. (5) is really the radius, so that the

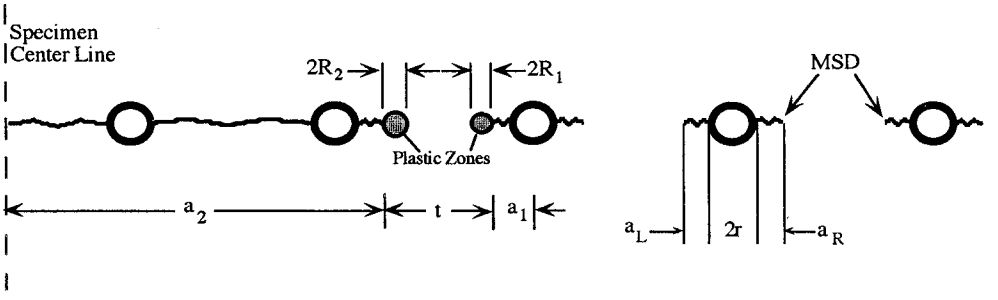

Fig. 2 Schematic representation of lead and MSD crack tip plastic zones used for ligament yield RS criterion.

plastic zone is actually twice as large as originally proposed by Irwin. The current authors have employed this latter plastic zone model in their interpretation of Swift's ligament yield criterion. To obtain Swift's original criterion, the 2s should be eliminated from Eq. (4), and subsequent equations modified accordingly.

Substituting Eq. (5) for R_1 and R_2 into Eq. (4) yields the following expression:

$$t = 2[(1/2\pi)(K_2/\sigma_{\text{flow}})^2 + (1/2\pi)(K_1/\sigma_{\text{flow}})^2] \quad (6)$$

This equation may be simplified to

$$\pi(\sigma_{\text{flow}})^2 t = (K_2)^2 + (K_1)^2 \quad (7)$$

As described in Refs. 2 and 5, K_1 for the MSD crack tip can be approximated by Eq. (8):

$$K_1 = [(P/BW_{\text{net}})]\sqrt{\pi a_1}\beta_h\beta_{i1} \quad (8)$$

Here, P is the remotely applied tensile load, B is the specimen thickness, and W_{net} is the net width of the specimen at the row of holes given by Eq. (9):

$$W_{\text{net}} = W - nd - 2n_{\text{msd}}L \quad (9)$$

In Eq. (8) β_{i1} is the stress intensity factor coefficient for crack 1 in Fig. 2 because of the interaction with the central lead crack, and is given in Refs. 3 and 4. The stress intensity factor coefficient β_h for a radial crack at a hole in Eq. (8) is also given in Refs. 3 and 4. Similarly, the stress intensity factor at the central lead crack tip can be approximated by Eq. (10):

$$K_2 = [(P/BW_{\text{net}})]\sqrt{\pi a_2}\beta_{i2} \quad (10)$$

Here, β_{i2} is the stress intensity factor coefficient for the central lead crack in Fig. 2 caused by the interaction with MSD crack 1, and is given in Refs. 3 and 4.

Substituting Eqs. (8) and (10) for K_1 and K_2 in Eq. (7) leads to the following expression:

$$\pi(\sigma_{\text{flow}})^2 t = \left(\frac{P}{BW_{\text{net}}}\right)^2 \beta_h^2 \pi a_1 \beta_{i1}^2 + \left(\frac{P}{BW_{\text{net}}}\right)^2 \pi a_2 \beta_{i2}^2 \quad (11)$$

Equation (11) can be simplified to

$$(\sigma_{\text{flow}})^2 t = \left(\frac{P}{BW_{\text{net}}}\right)^2 (a_1\beta^{2h}\beta_{i1}^2 + a_2\beta_{i2}^2) \quad (12)$$

Finally, solving Eq. (12) for P, and defining this load as P_{CLY}, yields the ligament yield failure load for specimens with MSD:

$$P_{\text{CLY}} = \sigma_{\text{flow}} BW_{\text{net}} \left[\frac{t}{(a_1\beta_h^2\beta_{i1}^2 + a_2\beta_{i2}^2)}\right]^{1/2} \quad (13)$$

Before applying the ligament yield model to the experiments, it would be helpful to review the assumptions in Eq. (13). First, since the Irwin plastic zone model assumes elastic–perfectly plastic behavior, and the 2024-T3 test material exhibits strain hardening, the Irwin plastic zone is computed here with the flow stress, which is defined as the average of the yield and tensile stress. Next the model ignores subcritical crack growth before link-up. As discussed in the following sections, however, this model did give a good estimate for the RS of the MSD panels.

Experimental Program

This section describes experiments conducted to measure the influence of MSD on lead crack RS and to evaluate the failure criteria described in the previous section. The 2024-T3 (bare) material used for the RS tests described here, and for the MSD fatigue tests described in Ref. 3, was obtained commercially in two separate lots consisting of four 2.3-mm- (0.09-in.-) thick panels that were originally 1.2 m (4 ft) wide and 3.7 m (12 ft) long.

Tensile Tests

Four tensile tests with the specimens oriented in the transverse–longitudinal (TL) direction (same as the MSD tests) were conducted to determine the yield stress σ_{ys} and ultimate stress σ_u for the 2024-T3 aluminum test material. An MTS tensile test machine with MATE software conforming with ASTM specification E-8[12] was used to apply a uniaxial, static load to dogbone tensile specimens. An extensometer was used to measure the strain as the change in length across a 1-in. span, and each specimen was loaded to failure in load control. The stress–strain curves from these tests are given in Fig. 3. The 0.2% offset σ_{ys} was determined to be 303 MPa (44.0 ksi) and σ_u was found to be 434 MPa (63 ksi).

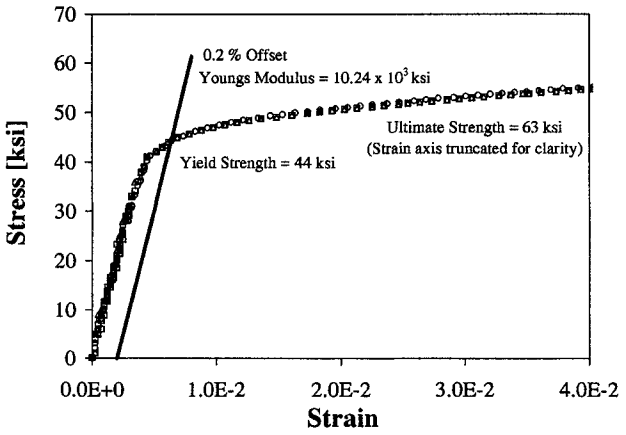

Fig. 3 Tensile stress–strain curves obtained for the 2024-T3 aluminum test material.

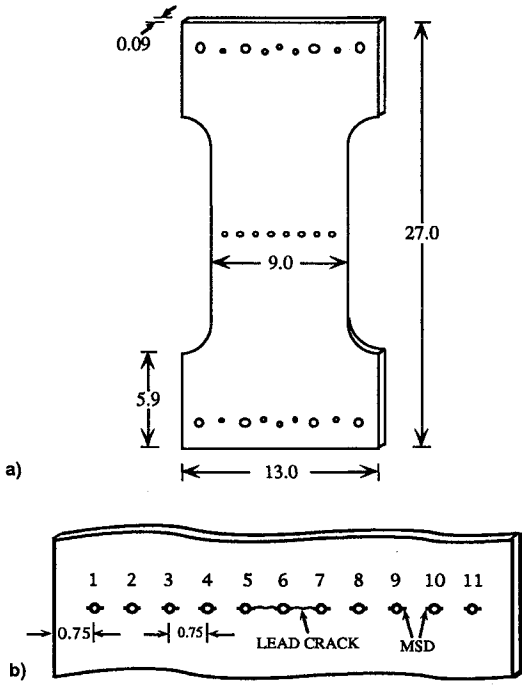

Fig. 4 Typical RS specimen (RS-01) with nominal 0.16-in. hole diameter: a) global specimen configuration (dimensions in inches) and b) detailed view of crack plane showing hole, lead crack, and MSD locations (dimensions in inches).

Residual Strength

Residual strength (RS) specimens with the dimensions shown in Fig. 4 were prepared to demonstrate the effects MSD cracks have on panel strength and to provide a comparison with RS predictions made by the criteria discussed in the previous section. The first specimen type had MSD at each hole and a lead crack spanning the central set of holes (see Fig. 1a). The second type also had a central lead crack, but the other holes were all uncracked (Fig. 1b). The third specimen type had only the central lead crack and there were no other holes or notches in the panel (Fig. 1c). There were two sets of each of these latter RS specimens: one set with 6.1-cm- (2.4-in.-) long ($2a$) lead cracks and another set with 8.1-cm- (3.2-in.-) long lead cracks. The type 3 specimens shown in Fig. 1c (lead crack only) were used to measure K-apparent.

The specimens were prepared by shearing the sheets of 2.3-mm- (0.09-in.-) thick 2024-T3 aluminum to a length of 68.6 cm (27 in.) and a width of 33 cm (13 in.). These sheets were flattened using a mechanical roller to remove slight warping present in the original 1.2 × 2.7 m (4 × 12 ft) sheets. Next, a 20-cm- (8-in.-) wide section across the center span of one side of the specimen was polished to a mirror-like finish to aid in viewing the cracks with an optical microscope. The sheet was then milled to the design specification using the abrasive jet described in Refs. 3 and 4. Small fatigue starter-notches (1.0 mm = 0.04 in. long by 0.25 mm = 0.01 in. wide) were cut at both sides of MSD holes with the abrasive jet.

Each specimen was precracked under constant amplitude cyclic loading until measurable cracks were visible under the optical microscope at both sides of all holes with starter notches. When precracking was complete, the abrasive jet was used to mill-out the starter notches and cut the holes to their final diameters (from a nominal diameter of 2.0 mm = 0.08 in. to a final nominal diameter of 4.1 mm = 0.16 in.). When this process was complete, the starter notches were removed, leaving only the fatigue cracks emanating from the hole edges. Each specimen was then carefully measured with a digital micrometer and optical microscope. Table 1 summarizes the dimensions and average crack length measurements for each RS specimen while Tables 2 and 3 provide the individual crack length measurements.

The crack opening displacement for the center lead crack was measured across the center of the crack at appropriate loading intervals for 11 of the RS specimens. These measurements were made with a clip gauge extensometer (MTS model 632.03 B-30) mounted between two small brackets located

Table 1 Measured dimensions of RS specimens

Specimen ID	Lead crack length a, in.	Average hole diameter, in.	Average MSD crack length measured from hole edge, in.	Number of holes with MSD cracks
RS-01a	1.240	0.140	0.043	6
RS-01b	1.215	0.156	0.021	6
RS-01c	1.232	0.162	0.071	6
RS-02a	1.244	0.142	No MSD	0
RS-03a	1.238	No holes	No holes	0
RS-03b	1.232	No holes	No holes	0
RS-04a	1.596	0.149	0.101	6
RS-04b	1.618	0.158	0.062	6
RS-04c	1.602	0.159	0.066	6
RS-04d	1.645	0.158	0.066	6
RS-05a	1.642	0.149	No MSD	0
RS-05b	1.626	0.160	No MSD	0
RS-06a	1.608	No holes	No holes	0
RS-06b	1.609	No holes	No holes	0

Note: The lead crack dimension a reported is half the total length ($2a$) for central lead cracks. Average MSD crack length is measured from edge of hole.

Table 2 Individual MSD crack lengths for RS specimens RS-01 to RS-03

Hole no.	Crack tip	Crack length a, in.					
		RS-01a	RS-01b	RS-01c	RS-02a	RS-03a	RS-03b
1	a_L	0.020	0.014	0.055	0.000	*	*
1	a_R	0.055	0.030	0.034	0.000	*	*
2	a_L	0.070	0.010	0.059	0.000	*	*
2	a_R	0.019	0.010	0.020	0.000	*	*
3	a_L	0.064	0.039	0.060	0.000	*	*
3	a_R	0.074	0.048	0.021	0.000	*	*
4	a_L	——	——	——	——	——	——
4	a_R	——	——	——	——	——	——
5	a_L	——	——	——	——	——	——
5	a_R	——	——	——	——	——	——
6	a_L	——	——	——	——	——	——
6	a_R	——	——	——	——	——	——
7	a_L	——	——	——	——	——	——
7	a_R	——	——	——	——	——	——
8	a_L	0.036	0.029	0.082	0.000	*	*
8	a_R	0.057	0.024	0.020	0.000	*	*
9	a_L	0.020	0.015	0.106	0.000	*	*
9	a_R	0.046	0.008	0.100	0.000	*	*
10	a_L	0.026	0.009	0.169	0.000	*	*
10	a_R	0.033	0.016	0.126	0.000	*	*

Note: Crack lengths a_R and a_L are measured from hole edge as defined in Fig. 2. Dashed lines represent cracks that are part of the lead crack reported in Table 1, whereas * indicates no holes or cracks present at this location.

Table 3 Individual MSD crack lengths for RS specimens RS-04 to RS-06 measured from the hole edge

Hole no.	Crack tip	Crack length a, in.							
		RS-04*a*	RS-04*b*	RS-04*c*	RS-04*d*	RS-05*a*	RS-05*b*	RS-06*a*	RS-06*b*
1	a_L	0.191	0.014	0.100	0.014	0.000	0.000	*	*
1	a_R	0.205	0.010	0.115	0.005	0.000	0.000	*	*
2	a_L	0.163	0.014	0.055	0.053	0.000	0.000	*	*
2	a_R	0.152	0.010	0.053	0.054	0.000	0.000	*	*
3	a_L	0.154	0.015	0.039	0.087	0.000	0.000	*	*
3	a_R	0.014	0.025	0.050	0.107	0.000	0.000	*	*
4	a_L	—	—	—	—	—	—	—	—
4	a_R	—	—	—	—	—	—	—	—
5	a_L	—	—	—	—	—	—	—	—
5	a_R	—	—	—	—	—	—	—	—
6	a_L	—	—	—	—	—	—	—	—
6	a_R	—	—	—	—	—	—	—	—
7	a_L	—	—	—	—	—	—	—	—
7	a_R	—	—	—	—	—	—	—	—
8	a_L	—	—	—	—	—	—	—	—
8	a_R	—	—	—	—	—	—	—	—
9	a_L	0.049	0.057	0.133	0.133	0.000	0.000	*	*
9	a_R	0.025	0.036	0.103	0.107	0.000	0.000	*	*
10	a_L	0.073	0.101	0.067	0.078	0.000	0.000	*	*
10	a_R	0.076	0.129	0.059	0.082	0.000	0.000	*	*
11	a_L	0.052	0.163	0.006	0.030	0.000	0.000	*	*
11	a_R	0.056	0.165	0.015	0.041	0.000	0.000	*	*

Note: Crack lengths a_R and a_L are measured from hole edge as defined in Fig. 2. Dashed lines represent cracks that are part of the lead crack reported in Table 2, whereas * indicates no holes or cracks at this location.

Table 4 Summary of measured and predicted failure loads for RS specimens

Specimen	MSD and holes	Lead crack length $2a$, in.	Measured load, kips	Calculated load, kips			Difference, %		
			$P_{C\,\text{actual}}$	$P_{C\,\text{net}}$	P_{CLY}	$P_{C\,\text{Kapp}}$	$P_{C\,\text{net}}$	P_{CLY}	$P_{C\,\text{Kapp}}$
RS-01*a*	MSD	2.4	20.20	19.51	20.86	26.69	3.42	3.27	32.13
RS-01*b*	MSD	2.4	23.25	20.40	22.74	27.33	12.26	2.19	17.55
RS-01*c*	MSD	2.4	19.82	17.80	19.42	26.90	10.19	2.02	35.72
RS-02*a*	No MSD	2.4	25.55	22.42	n/a	27.67	12.25	n/a	8.30
RS-03*a*	No holes	2.4	27.95	24.97	n/a	28.20	10.66	n/a	0.89
RS-03*b*	No holes	2.4	28.46	25.97	n/a	28.31	9.10	n/a	0.53
RS-04*a*	MSD	3.2	12.91	14.01	17.70	22.63	8.52	37.10	75.29
RS-04*b*	MSD	3.2	17.15	15.41	17.83	22.63	10.15	3.97	31.95
RS-04*c*	MSD	3.2	16.26	15.30	16.02	21.78	5.90	1.48	33.95
RS-04*d*	MSD	3.2	15.59	15.01	14.99	21.13	3.72	3.85	35.54
RS-05*a*	No MSD	3.2	21.73	19.10	n/a	23.08	12.10	n/a	6.21
RS-05*a*	No MSD	3.2	21.81	18.61	n/a	23.08	14.67	n/a	5.82
RS-06*a*	No holes	3.2	23.64	22.90	n/a	23.93	3.13	n/a	1.23
RS-06*b*	No holes	3.2	23.95	22.14	n/a	23.93	7.56	n/a	0.08

Note: Percent difference is based on comparison of calculated and measured load. The term no holes means specimen contained no holes or cracks other than central lead crack.

above and below the central lead crack. The brackets had knife edges, and were glued to the specimens at a spacing of 6.4 mm (0.25 in.) with 5-min epoxy.

Each RS specimen was statically loaded to fracture in uniaxial tension using a 200-kip capacity servohydraulic testing machine. Applied load and crack opening displacement data were obtained at appropriate load intervals. The measured loads at fracture $P_{C\,\text{actual}}$ are given in Table 4 along with the residual strengths computed by the three methods described in the previous section. Those data are discussed in the following section.

Discussion of Results

Four type 3 specimens (lead crack only) were tested to determine K_{app}. Two specimens each were tested with initial crack lengths $2a$ = 6.1 cm (2.4 in.) and 8.1 cm (3.2 in.). Failure loads are recorded in Table 4 for these tests, and give an average value of 78.9 MPa-m$^{1/2}$ (71.9 ksi-in.$^{1/2}$) for K_{app}. Individual values did not vary with crack length, with the two shorter crack length specimens giving K_{app} of 78.4 and 79.6 MPa-m$^{1/2}$ (71.4 and 72.5 ksi-in.$^{1/2}$), whereas the longer crack length tests gave apparent toughness values of 78.3 and 79.4 MPa-m$^{1/2}$ (71.3 and 72.3 ksi-in.$^{1/2}$).

The crack opening measurements were plotted as a function of the applied load to show the behavior of the crack as the load was increased. Figure 5 shows the crack opening displacement curves for the three types of RS specimens with 6.1-cm (2.4-in. total crack length) lead cracks. Figure 6 presents the data for the RS specimens with 8.1-cm (3.2-in. total crack length) lead cracks. The results are similar for the three specimen types during the initial loading (elastic/linear region), but each type behaves differently as the failure load is approached. For instance, type 1 specimens RS-01*a*, *b*, and *c* and RS-04*b*, *c*, and *d* (specimens with MSD) show little ductility, as the load-displacement curves remain essentially linear up to ultimate failure. In contrast, type 2 specimens RS-02*a* and RS-05*b* (specimens with holes but no MSD) show rapid crack opening just before failure, indicative of subcritical crack growth and significant plastic deformation. This nonlinear effect is even more pronounced for type 3 specimens RS-03*a* and *b* and RS-06*a* and *b* (no holes or MSD).

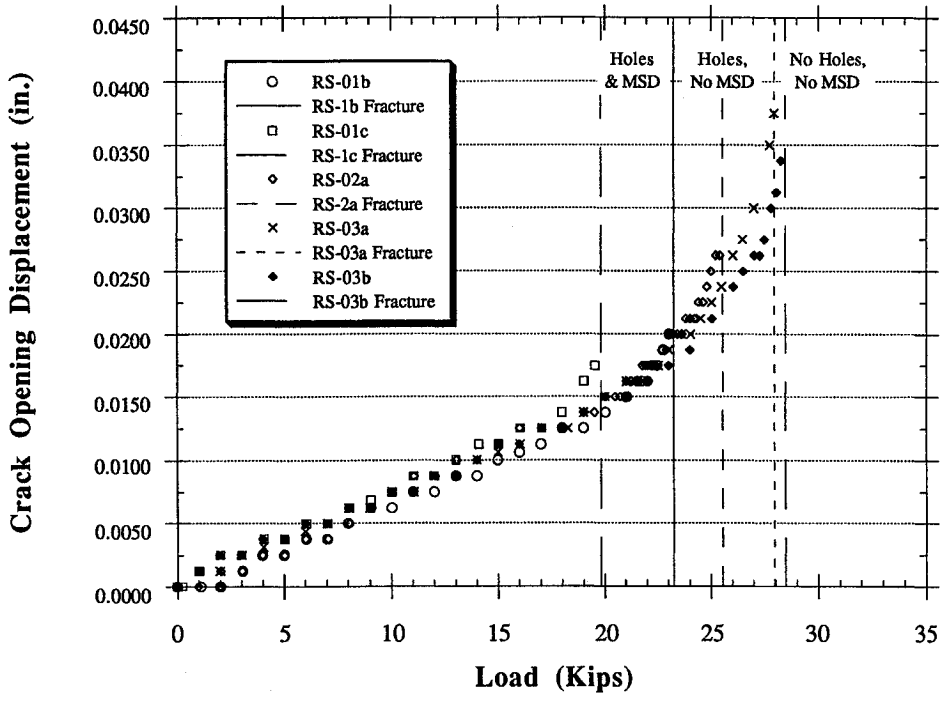

Fig. 5 Crack opening displacement curves for RS specimens with 2.4-in.-long (total length 2*a*) lead cracks.

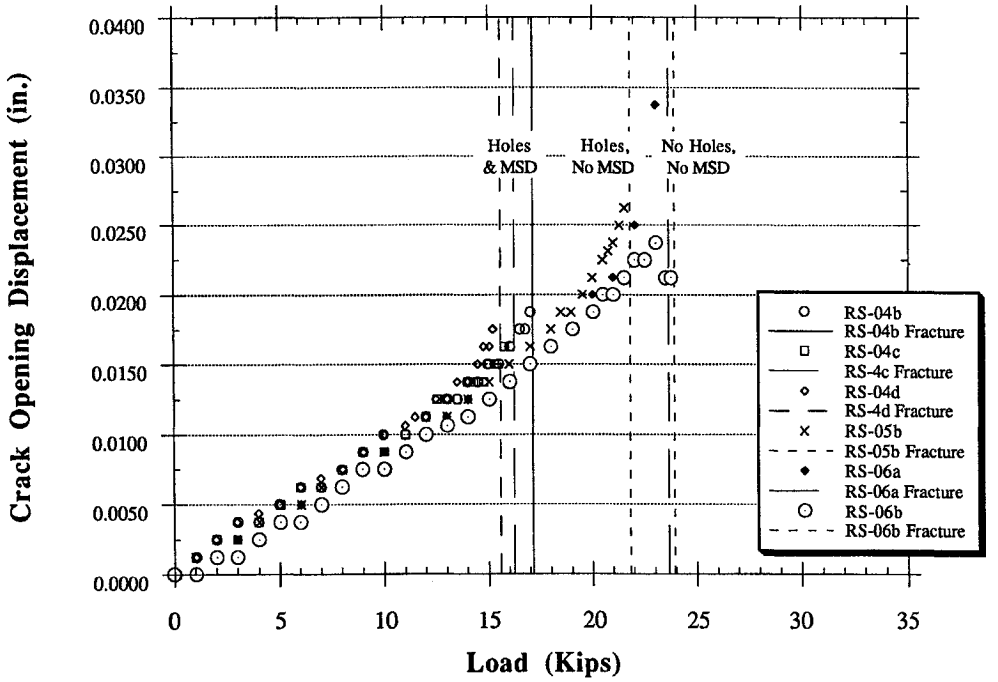

Fig. 6 Crack opening displacement curves for RS specimens with 3.2-in.-long (total length 2*a*) lead cracks.

Failure loads for the different specimens are also indicated on the crack opening displacement curves given in Figs. 5 and 6 to demonstrate the loss of strength in panels with holes and MSD. A comparison between panels with MSD (type 1 RS specimens) and similar panels without MSD (type 2 RS specimens) demonstrates the significant loss in RS caused by the MSD. This behavior is summarized graphically in Figs. 7 and 8. Note that the specimens listed in each figure have similar geometries and lead crack lengths. These specimens only differ in whether or not they have MSD at their holes.

The principal objective of the RS tests was to evaluate the three failure criteria for determining RS. The measured RSs in type 1 panels (those with MSD) are compared with the predicted values in Table 4 and Fig. 9. Note that the ligament yield criterion is the most accurate for panels with MSD, while the *K*-apparent predictions always overestimated the strength of panels when MSD was present. The net section yield criterion was generally conservative and gave acceptable results, although the ligament yield criterion was still better for all but one specimen (RS-04*a*). It can also be seen from Table 4 that the *K*-apparent method closely predicted the failure loads when no MSD was present. Based on the data given in Table 4, the average errors for the three residual strength failure criteria are as follows: for panels with MSD: ligament yield method, 7.7%; *K*-apparent method, 37.5%; and net section yield method, 7.8%. For panels without MSD: ligament yield method, not applicable; *K*-apparent method, 3.3%; and net section yield method, 14.1%.

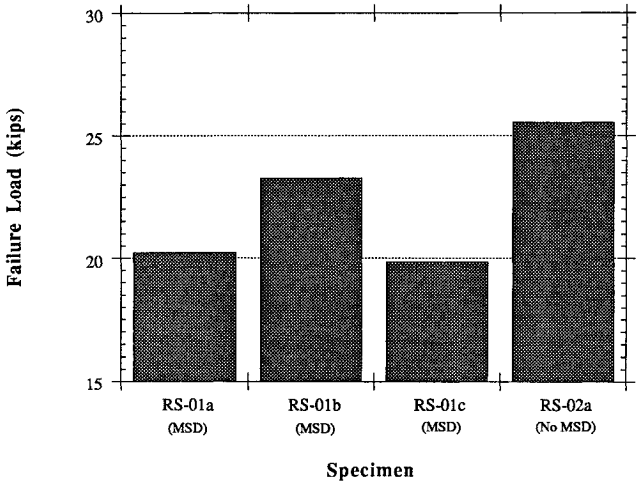

Fig. 7 Comparison of RS for specimens with 2.4-in. lead cracks showing effect of MSD on failure load.

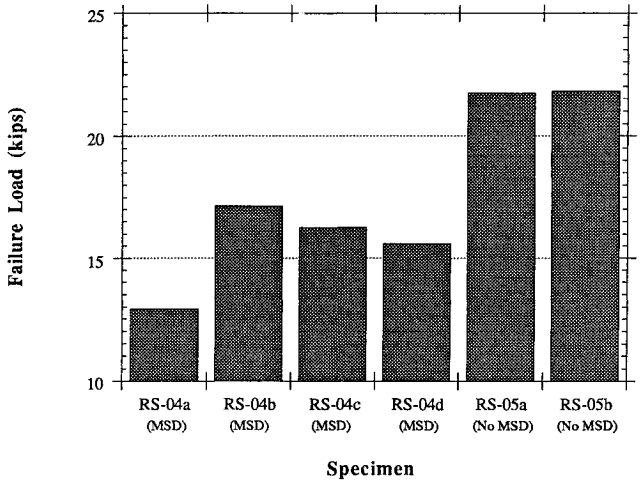

Fig. 8 Comparison of RS for specimens with 3.2-in. lead cracks showing effect of MSD on failure load.

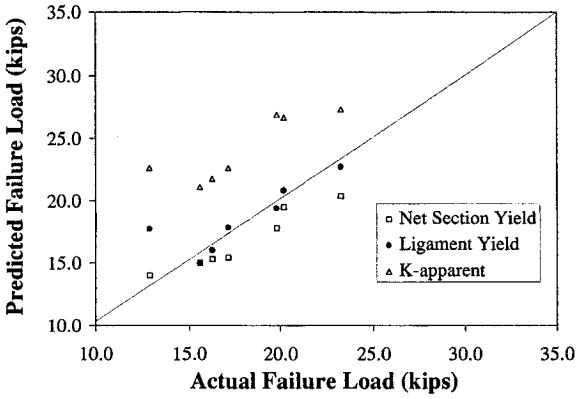

Fig. 9 Comparison of measured failure loads with various prediction criteria for type 1 RS specimens (those with MSD).

The ligament yield criterion proposed by Swift[2,5] predicted a failure load of 17.70 kips for specimen RS-04*a* when the actual failure load was measured as 12.91 kips (an error of 37.1%). This was the only MSD specimen for which the ligament yield criterion did not closely predict the failure load (the average error for the ligament yield criterion is only 2.8% when RS04*a* is not considered). A review of the individual crack lengths for specimen RS04*a* given in Table 3 reveals that this specimen did not have uniform MSD. The holes to the left of the central crack had relatively large cracks averaging 0.147 in., while the holes to the right had much smaller MSD cracks averaging 0.055 in. The ligament yield criterion assumes nearly uniform MSD on both sides of the central lead crack, and predicts failure when the plastic zones associated with the lead crack and the nearest MSD crack link-up. In the case of RS04*a*, the left side of the specimen was much weaker than the right side. As a result, the relatively large MSD cracks at the holes on the left side extended and linked-up with the lead crack before the ligament yield criterion would have predicted had there been relatively uniform MSD at the holes on both sides of the lead crack. The ligament yield and the net section yield criteria produced reasonably accurate predictions of failure loads for RS panels with MSD. The *K*-apparent method produced very good results when MSD was not present, but when MSD did exist, this method consistently overestimated the RS of the panels with MSD.

When the RS specimens were loaded to failure, little or no stable crack extension was observed with the naked eye prior to ultimate panel failure. Large elliptical-shaped areas of plastic deformation, however, were clearly visible at the crack tips, especially in front of the lead cracks, as the load approached the failure point. In general, the failure mode appeared to simulate the ligament yield failure criterion; the plastic zones grew to the point where the zone from the lead crack touched the zone from one of its neighboring MSD cracks. When this happened the crack extended rapidly and suddenly, and then the panel unzipped, failing completely across the midspan. This same phenomenon was also observed during the MSD cyclic fatigue tests[3] just prior to failure of the MSD specimens with lead cracks.

Conclusions

Fourteen aluminum panel specimens were tested to determine the static load they could bear before complete failure occurred from a large lead crack. The test results are compared with the failure loads predicted by three different methods of performing RS calculations for panels that contain MSD. The following conclusions can be drawn from the results of this research.

1) The presence of MSD in panels significantly reduces RS.

2) Predictions of RS that do not account for the effects of crack interaction and plasticity overestimate the strength of the panel and could result in nonconservative designs.

3) The ligament yield criterion produced good estimates of the RS of panels with a central lead crack and nearly uniform MSD. For panels without MSD, the *K*-apparent approach was suitable for the specimens examined here. The *K*-apparent method did not, however, yield good MSD RS predictions for the 2024-T3 panels examined here.

4) The net section yield criterion gave adequate and conservative results for the present MSD panels.

5) While the ligament yield and net section yield criteria performed well for the relatively small, unstiffened panels described here, these criteria should be subjected to further tests with larger specimens that more closely simulate the conditions in stiffened aircraft structure, and which also involve load transfer through the fastener holes.

Acknowledgments

The first author, Commander E. J. Moukawsher, died during the review process after this article was submitted for publication to the *Journal of Aircraft*. He is greatly missed by his friends and colleagues. The authors wish to thank the U.S. Coast Guard for providing the test materials and for supporting the graduate studies of E. J. Moukawsher at Purdue University. Portions of this research were sponsored by the U.S. Air Force Office of Scientific Research Grant F49620-93-1-0377. The assistance of M. Bowman who provided use of facilities of the

Purdue School of Civil Engineering for conducting the residual strength tests is also appreciated. The authors especially thank T. Swift of the Federal Aviation Administration for suggesting the ligament yield failure criterion and for his encouragement and advice during the course of the research.

References

[1]Hendricks, W. R. "The Aloha Airlines Accident—A New Era for Aging Aircraft," *Structural Integrity of Aging Airplanes*, edited by S. N. Atluri, S. G. Sampath, and P. Tong, Springer–Verlag, Berlin, 1991.

[2]Swift, T. "Widespread Fatigue Damage Monitoring Issues and Concerns," 5th International Conference on Structural Airworthiness of New and Aging Aircraft, Hamburg, Germany, June 1993.

[3]Moukawsher, E. J., Grandt, A. F., Jr., and Neussl, M. A., "Fatigue Life Panels with Multiple Site Damage," *Journal of Aircraft*, Vol. 33, No. 5, 1996, pp. 1003–1013.

[4]Moukawsher, E. J., "Fatigue Life and Residual Strength of Panels with Multiple Site Damage," M.S. Thesis, School of Aeronautics and Astronautics, Purdue Univ., West Lafayette, IN, May 1993.

[5]Swift, T., "Damage Tolerance Capability," *Fatigue of Aircraft Materials*, Proceedings of the Specialists Conferences, dedicated to the 65th birthday of J. Schijve, 1992, Delft Univ., Delft Univ. Press, Delft, The Netherlands, 1992, pp. 351–387.

[6]Newman, J. C., Jr., Dawicke, D. S., Sutton, M. A., and Bigelow, C. A., "A Fracture Criterion for Widespread Cracking in Thin-Sheet Aluminum Alloys," International Committee on Aeronautical Fatigue ICAF 17th Symposium, Stockholm, Sweden, June 1993.

[7]Schijve, J., "Multiple-Site Damage in Aircraft Fuselage Structures," Delft Univ. of Technology Rept. LR-729 (preliminary version), Delft, The Netherlands, July 1993.

[8]Broek, D., *Elementary Engineering Fracture Mechanics*, 3rd revised ed., Martin Nijhoff Publishers, Boston, MA, 1982.

[9]Mohaghegh M., and Axter, S. E., "Development of Optimum Materials for Aircraft Structures," AIAA Paper 90-1029, April 1990.

[10]"Metallic Materials and Elements for Aerospace Vehicle Structures," *Military, Standardization Handbook*, MIL-HBK-5E, Dept. of Defense, Defense Printing Service, Philadelphia, PA, June 1987.

[11]Rooke, D. P., and Cartwright, D. J., *Compendium of Stress Intensity Factor*, Her Majesty's Stationary Office, London, 1976.

[12]"Test Methods of Tension of Metallic Materials," American Society for Testing and Materials Specification E8-89, July 1991.